Pure & Appl. Chem., Vol. 62, No. 12, pp. 2287–2296, 1990.
Printed in Great Britain.

Molecular processes in electrolyte solutions at microwave frequencies

J.Barthel, R.Buchner, K.Bachhuber, H.Hetzenauer, M.Kleebauer and H.Ortmaier

Institut für Physikalische und Theoretische Chemie der Universität Regensburg, D-8400 Regensburg, Germany

Abstract - The microwave dispersion and absorption spectra are discussed for various protic and aprotic electrolyte solutions and their solvents over large frequency ranges, in general 0.9-90 GHz. Wider frequency ranges are covered for water (0.9-409 GHz) and for methanol, N-methylformamide, and N,N-dimethylformamide (all 0.9-293 GHz). The role of insufficient frequency coverage is critically discussed.

Permittivities and relaxation times of the underlying relaxation processes are compared for electrolyte solutions of the hydrogen-bonding solvents water, methanol and higher alcohols, formamide, N-methylformamide, and the dipolar aprotic solvents acetonitrile, propylene carbonate, dimethylsulfoxide, and N,N-dimethylformamide. The hydrogen-bonding mode at $\tau \approx 1$ ps is not affected by the addition of alkali metal and tetrabutylammonium salts, in contrast to the bulk and the internal relaxation of the H-bonded chains; NH_4^+ in methanol produces peculiar effects.

For 1:1-electrolytes ion-pair formation is detectable in all solvents of static permittivity below 50; the concentration dependence of the corresponding relaxation time permits separation into rotational and kinetic modes of ion-pair formation and decomposition.

INTRODUCTION

Dielectric relaxation studies on liquid systems are an efficient tool to investigate the structure of solutions and the dynamics of molecular interactions. Examples of application are the determination of orientation-correlation functions of simple dipolar liquids permitting the test of liquid state models [1] or the investigation of solvation dynamics and charge transfer kinetics [2]. Biochemistry is interested in the study of water/ion/biomolecule interactions [3,4]. Physical chemistry of electrolyte solutions receives a wealth of information on the effect of ion-ion, ion-solvent and solvent-solvent interactions on structure and dynamics [5,6,7]. In this contribution recent results of systematic studies on aqueous and non-aqueous electrolyte solutions are reported revealing the broadness of cognition about such systems available from a sufficiently large frequency coverage in the microwave range, but also pinpointing common features of different solvent classes.

FREQUENCY DEPENDENCE OF PERMITTIVITY AND ELECTRIC POLARIZATION

Dielectric relaxation data are obtained from the application of a time-dependent electric field to a sample and registration of its response to the perturbation which is given by the Maxwell relations. The observable quantity is the electric polarization

$$\vec{P}(t) = \varepsilon_o(\varepsilon - 1) \cdot \vec{E}(t) \qquad (1)$$

where ε_o and ε are the permittivity of the vacuum and the relative permittivity of the sample, respectively; $\vec{E}(t)$ is the strength of the applied electric field.

At molecular level $\vec{P}(t)$ is the consequence of two effects. A first contribution to $\vec{P}$, called orientational polarization $\vec{P}_\mu$, stems from the alignment of the permanent molecular dipole moments $\vec{\mu}_i$ which are orientated in the applied field against thermal motion. The motion of charged particles affecting the electroneutrality of the solution, and effects arising from chemical reactions which involve dipole moment changes are subsumed to this contribution. The second contribution to $\vec{P}$, called induced polarization $\vec{P}_\alpha$, stems from the induction of a dipole moment $\vec{\mu}_{i,ind}$ in every molecule of type i due to its polarizability α_i: $\vec{\mu}_{i,ind} = \alpha_i \vec{E}$. It is generally assumed that $\vec{P}_\mu$ and $\vec{P}_\alpha$ are linearly independent. $\vec{P}_\alpha$ follows changes of the field $\vec{E}(t)$ without delay in the time scale of dielectric experiments up to far-infrared frequencies, in contrast to $\vec{P}_\mu$. Therefore the induced contribution can be characterized at microwave fre-

quencies by a constant quantity, the so-called infinite frequency permittivity ε_∞(s.eq.(2a)). The time evolution of $\vec{P}_\mu(t)$ (s.eq.(2b)), and hence also that of $\vec{P}(t)$ is characteristic for molecular reorientation, charge migration, and chemical reactions in the liquid.

$$\vec{P}_\alpha = \varepsilon_o(\varepsilon_\infty - 1)\vec{E}\,; \qquad \vec{P}_\mu = \varepsilon_o(\varepsilon - \varepsilon_\infty)\vec{E} \tag{2a,b}$$

Two experimental approaches are possible to the search of information, time- and frequency-domain methods. For either method experimental difficulties arise from the time scale for molecular motions in liquids, ranging from about 0.1 ps to several nanoseconds. This interval corresponds to frequencies in the microwave region from a few megahertz to several terahertz. Figure 1 informs about frequency regions and respective processes contributing to the permittivity of electrolyte solutions and their solvents.

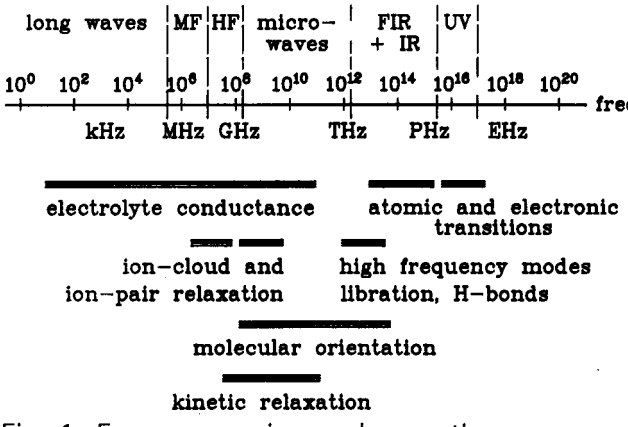

Fig. 1. Frequency regions and respective processes contributing to the permittivity of liquids and solvents.

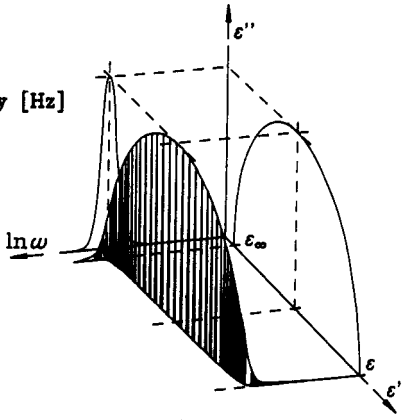

Fig. 2. Spatial (ε',ε'',lnω)-diagram and its (ε',lnω)-, (ε'',lnω)- and (ε'',ε')-projections [6].

In a time-domain experiment a field jump is applied to the sample at time t_o=0. The orientational polarization of the sample relaxes to its new equilibrium, controlled by a step response function $F_p^{or}(t)$

$$\vec{P}_\mu(t) = \vec{P}_\mu(0)\cdot F_p^{or}\,; \qquad F_p^{or} = \frac{\langle \vec{P}_\mu(0)\cdot\vec{P}_\mu(t)\rangle}{\langle \vec{P}_\mu(0)\cdot\vec{P}_\mu(0)\rangle} \tag{3a,b}$$

The response function is characteristic for the underlying processes. In the case of a first order law for the polarization decay

$$-\frac{d\vec{P}_\mu}{dt} = \frac{\vec{P}_\mu}{\tau}\,; \qquad \vec{P}_\mu(t) = \vec{P}_\mu(0)\cdot\exp(-\frac{t}{\tau}) \tag{4a,b}$$

this is the exponential decay function $F_p^{or}(t) = \exp(-t/\tau)$ with relaxation time τ. Usually, however, more complicated functions are found which must be deconvoluted into normal modes.

Obviously, the step response function, by its definition, eqs.(3), concerns a phase property, namely the polarization $\vec{P}_\mu(t)$ of the sample; the corresponding macroscopic relaxation time τ is related to the reorganization of the phase structure after a perturbation. The study of molecular processes requires microscopic (molecular) relaxation times τ'; for dipole reorientation the microscopic relaxation time τ' is defined by the orientational correlation function

$$\phi(t) = \frac{\langle \vec{\mu}(0)\cdot\vec{\mu}(t)\rangle}{\langle \vec{\mu}(0)\cdot\vec{\mu}(0)\rangle} = \langle\cos\theta(t)\rangle \tag{5}$$

Actually there is no satisfactory general theory permitting the conversion of measured relaxation times τ_j to molecular relaxation times τ'_j. The estimation of the cross-correlation effects due to the long-range nature of dipole-dipole interactions, necessary for a proper conversion of F_p^{or} to ϕ, is still a matter of discussion. In cases where the reorientation of the molecular dipole moment can be described by a rotational diffusion motion, the molecular relaxation time can be approximated with the help of the Powles-Glarum relation

$$\tau' = \frac{2\varepsilon + \varepsilon_\infty}{3\varepsilon}\cdot\tau \tag{6}$$

There is no experimental technique permitting the direct measurement of $\vec{P}(t)$ by time-domain measurements, so that apparatus functions, depending on the experimental arrangement must be taken into account. A lucid introduction to the basic principles and problems of dielectric time-domain spectroscopy (TDS) is given by Cole [8], recent developments can be found in ref.[9]. With modern equipment, dielectric spectra in the range from 10 MHz to 10 GHz can be recorded within a few minutes with an accuracy of several percent.

Frequency-domain methods probe relaxation processes by the application of harmonic fields $\vec{E}(t)=\vec{E}_o \exp(i\omega t)$, of frequency ν, $\omega = 2\pi\nu$. Dielectric relaxation leads to amplitude reduc-

tion and phase shift of the propagating wave and hence of the frequency-dependent orientational polarization of the sample. A frequency-dependent complex permittivity $\hat{\varepsilon}(\nu)$ is used to describe the dissipative process; $\hat{\varepsilon}(\nu)=\varepsilon'(\nu)-i\varepsilon''(\nu)$ is related to the negative time derivative of the step response function, called pulse-response function $f_p^{or}(t)=(-\partial F_p^{or}(t)/\partial t)$, via Laplace transformation

$$\hat{\varepsilon}(\nu) = (\varepsilon - \varepsilon_\infty) \int_0^\infty f_p^{or}(t) \cdot e^{-i\omega t}\, dt \tag{7}$$

The first order process, eqs.(3), $f_p^{or} = \tau^{-1}\exp(-t/\tau)$, yields the Debye equation

$$\hat{\varepsilon}(\nu) = \varepsilon_\infty + \frac{\varepsilon - \varepsilon_\infty}{1 + i\omega\tau} \tag{8}$$

which is representable (Fig.2) by a three dimensional curve $(\varepsilon',\varepsilon'',\nu)$ or its projections in the (ε',ν)-plane, the dispersion curve, in the (ε'',ν)-plane, the absorption (loss) curve, and in the $(\varepsilon',\varepsilon'')$-plane, the Argand diagram. In Fig.2 $(\varepsilon-\varepsilon_\infty)$ is the dispersion amplitude of the process; its relaxation time is calculable from the frequency at the maximum of the absorption curve or the frequency at the inflection point of the dispersion curve.

To deal with more complicated relaxation behaviour, splitting of the experimental complex permittivity spectrum into a suite of distinct relaxation processes is attempted. It may be necessary to use empirical relaxation-time distribution functions, such as the Cole-Cole ($0\leq\alpha<1$, $\beta=1$) or the Cole-Davidson ($\alpha=0$, $0<\beta\leq1$) equation to fit individual components (cf.ref.[10]).

$$\hat{\varepsilon}(\nu) = \varepsilon_\infty + (\varepsilon - \varepsilon_\infty) \sum_{j=1}^{n} \frac{g_j}{[1 + (i\omega\tau_j)^{1-\alpha_j}]^{\beta_j}} \tag{9a}$$

Here n is the number of separable dispersion steps j of relaxation time τ_j and weight

$$g_j = \frac{\varepsilon_j - \varepsilon_{\infty j}}{\varepsilon - \varepsilon_\infty}, \quad \varepsilon_{\infty j} = \varepsilon_{j+1} \tag{9b,c}$$

contributing to the total dispersion from the static value $\varepsilon=\varepsilon_1$ to $\varepsilon_\infty=\lim_{\nu\to\infty}\varepsilon'$.

The parameters $\alpha_j>0$ and $\beta_j<1$ describe either a symmetric or asymmetric distribution of relaxation times for process j. In our experience it is always possible to fit such a semi-empirical relaxation model to experimental spectra, provided librational and inertial effects do not contribute appreciably, i.e. ν should not exceed 300-500 GHz. Admittedly, such models cannot always claim a physical basis.

EXPERIMENTAL METHODS AND DEVICES

There is a variety of methods for the determination of complex permittivities in the frequency domain; a review is given by Kaatze and Giese [11]. A drawback of all devices is the limited frequency coverage. True broad band experiments can only be performed in the far-infrared for frequencies above 300 GHz (5 cm^{-1}) using dispersive Fourier transform spectrometry (DFTS) [12], and on the low frequency side with time domain spectroscopy (TDS) or newly emerging vector network analyzer techniques [13]. Actually the gap between about 10 GHz and 300 GHz must be bridged by conventional microwave equipment based on waveguides to get high quality data. Here, the major inconvenience is the limited range of frequencies transmissable in a specified waveguide. In the authors' laboratory a set up of five waveguide and one coaxial apparatus is used to cover the frequency range from 0.9 to 89 GHz. Difficulties also arise from machining the cell and the necessary surroundings with sufficient accuracy. This is especially true for $\nu>50$ GHz.

Due to the demanding technical problems, complex permittivity measurements at intermediate frequencies, between 20 GHz and 300 GHz are scarce. However, there is an increased interest in this region since in the corresponding time scale, 0.5-5 ps, the transition occurs from fast librational motions to the slow diffusive mode; inertial effects should contribute to the spectra, and fast processes connected with hydrogen-bond dynamics or intramolecular reorientation take place. For liquids of molecules with high dipole moment, such as methyl chloride, also an excess absorption was found, which is not understood at the moment [14,15].

For electrolyte solutions the ohmic current, characterized by the specific conductance at static fields, κ, poses an additional problem in the determination of complex permittivities. From the solution of Maxwell's equations follows that only a generalized complex permittivity $\hat{\eta}(\nu)$ is experimentally accessible. $\hat{\eta}$ summarizes the effects of ohmic and displacement currents, which both depend on the frequency of the electric field.

$$\hat{\eta}(\nu) = \hat{\varepsilon}(\nu) + \frac{i\,\hat{\kappa}(\nu)}{2\pi\nu\varepsilon_o} \tag{10}$$

However, the dispersion of conductivity is very small. Actually, for the lack of better information, the generally accepted procedure to separate $\hat{\eta}(\nu)$ is to assume frequency independent conductivities, $\kappa'(\nu)=\kappa$ and $\kappa''(\nu)=0$, so that

$$\eta'(\nu) = \varepsilon'(\nu); \qquad \eta''(\nu) = \varepsilon''(\nu) + \frac{\kappa}{2\pi\nu\varepsilon_o} \tag{11a,b}$$

The static conductivity κ can either be treated as an adjustable parameter or, as it is done in our laboratory, determined in a separate experiment with high precision (<0.1 %) [18]. Due to the proportionality in ν^{-1}, the conductivity term poses a severe problem for the determination of ε'' at low frequencies, as it can be seen in Fig.3.

In the authors' laboratory the equipment covering the range 0.95-89 GHz, based on the method of travelling waves, is optimized for the high dielectric losses commonly found in electrolyte solutions [7,16]. It was successfully used to study systems with static permittivities ranging from 186 (N-methylformamide) down to 7 (in methanol/tetrachlormethane-mixtures). For frequencies up to 40 GHz, the accuracy is better than 1.5 % for η' and 2.5 % for η''; for the E-Band machine (60-90 GHz) approximately 3 %, depending somewhat on the system studied, is realistic for both η' and η''. The time window accessible with this equipment is from about 1.5 ps to 200 ps, if no additional information from other sources is available, but reasonable relaxation parameters up to 360 ps and down to 0.7 ps could be extracted in favourable cases [19,20].

ACCESSIBLE FREQUENCY RANGE AND RELAXATION MODEL

From the preceding discussion it is evident that the frequency range accessible to the experiment will critically affect the choice of the relaxation model, which is suitable to fit the data. This is exemplified for methanol in Table 1 which summarizes the results obtained in our laboratory with increasing frequency coverage. The second column of the table shows the relaxation model which yields the best fit of the data between 0.95 GHz and the upper frequency ν_{max}. In Fig.4 the loss curves calculated with the parameters of Table 1 are compared with the experimental data.

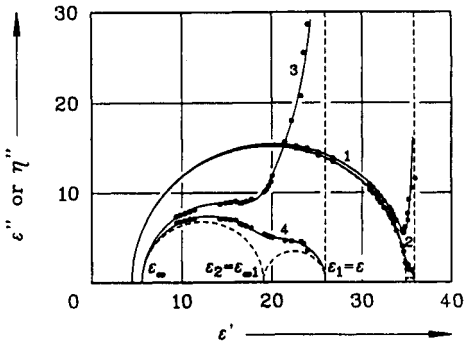

Fig. 3. Argand diagrams of 0.06 M (curves 1, 2) and 1.38 M (curves 3,4) solutions of Bu_4NBr in acetonitrile [17]. Curve 1 and 3 show the experimentally accessible data η'' vs. ε'; curves 2 and 4 are the corresponding diagrams ε'' vs. ε' after conductance correction (eqs.(11)). The broken lines (from left to right) are the individual contributions of solvent or ion-pair relaxation and conductance.

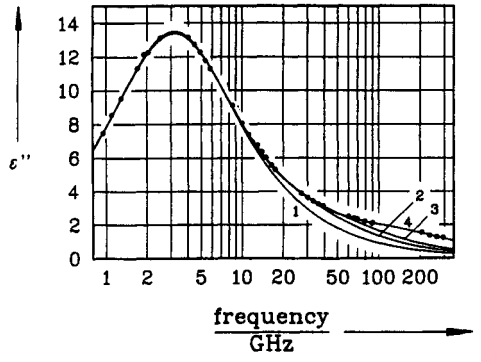

Fig. 4. Experimental loss data (•) of methanol at 25°C and spectra (curves 1 to 4) calculated with the parameters of Table 1. For explanation see text.

Obviously, the number of dispersion steps increases from n=1 to n=3 with increasing ν_{max}. This is not necessarily a criterion for the approach to the "true" relaxation behaviour. Table 1 shows that the dispersion amplitudes $\Delta\varepsilon_j=\varepsilon_j-\varepsilon_{j+1}$ of the fast processes, j=2,3, are small compared to the dominating slow process and the difference between the relaxation frequencies, $\nu_j=1/(2\pi\tau_j)$, is comparable to the half-widths of the corresponding loss curves. In such a situation the result of the fit, especially for the intermediate dispersion step, critically depends on the quality of the data.

From the pioneering work of Garg and Smyth [23] it is known that the higher linear alcohols (1-propanol to 1-dodecanol) exhibit three distinct dispersion steps. Such a behaviour is also found for ethanol and 2-propanol where the parameters also show a reasonable dependence on chain-length [19]. One may argue whether the use of Debye equations up to 10 cm^{-1} is possible; irrespective to this doubt, the fit allows a continuous match of microwave and far-infrared data, as shown in Fig.4. No further relaxation process is probable in the frequency range studied. The small discrepancy between the zero-frequency permittivity of the 3-Debye fit, ε=32.50, and the static permittivity value of methanol determined with conventional techniques, ε_s=32.63 [18], could be an indication for a small relaxation time distribution for the main dispersion step. However, this small effect can only be clarified by additional experiments below 0.9 GHz. A serious argument for the assumption of three dispersion steps of Debye type for methanol is, that only this model permits a consistent interpretation of electrolyte data [16].

Table 1: Dielectric relaxation parameters of methanol at 25° C

curve	model	ε	τ_1 / ps	ε_2	τ_2 / ps	ε_3	τ_3 / ps	ε_∞	ν_{max} / GHz	ref.
1	Cole-Cole	32.64	50.2*					5.27	12	[21]
2	2 Debye	32.49	51.4	5.89	5.2			4.07	18	[5]
3	2 Debye	32.47	51.0	5.74	3.3			3.68	40	[6]
4	3 Debye	32.50	51.5	5.91	7.09	4.90	1.12	2.79	293†	[19]

* $\alpha_1 = 0.014$ † including far-infrared data from ref.[22]

Table 1 shows that the parameters ε and τ_1 of the main dispersion step of pure methanol do not change appreciably with the number of relaxation processes. For electrolyte solutions the situation is different. In the case NaBr in methanol, for instance, the dielectric decrement $\delta_\varepsilon = -\lim_{c\to 0}(d\varepsilon_s/dc)$, showing the initial slope of the solvent permittivity ε_s plotted vs. c (c electrolyte concentration), remains constant at $\delta_\varepsilon = (42 \pm 2)$ dm mol^{-1}, whereas for $NaClO_4$ the decrement shifts from $\delta_\varepsilon = 41$ dm mol^{-1} to $\delta_\varepsilon = (33.1 \pm 1.3)$ dm mol^{-1} when going from a Cole-Cole fit up to 12 GHz to a 3-Debye fit up to 89 GHz. This discrepancy must be considered when δ_ε-results from experiments with different frequency coverage are compared in a discussion on solvation and kinetic depolarization. Analogous considerations apply for the relaxation times.

RELAXATION MODEL AND SOLVENT STRUCTURE

A possible interpretation of the relaxation behaviour of methanol is suggested by the structure of the liquid, which is dominated by winded chains of hydrogen-bonded molecules [19]. The fast time constant, τ_3, is related to the dynamics of the hydrogen bond and originates from a flipping motion of "free" OH groups between two acceptor sites and/or the breaking and reforming of a given bond in a translational motion. Indeed for methanol a hydrogen-bond lifetime in the order of 1 to 2 ps is suggested by molecular dynamics simulations of Haughney et al. [24]. τ_2 is compatible with the reorientation of single alcohol molecules at the chain ends and/or monomers. This is supported by NMR experiments which yield a characteristic time for the rotational motion of 6.6 ps [25], whereas 10.2 ps are obtained with quasielastic neutron scattering [26]. The main relaxation process with the relaxation time τ_1, is cooperative in nature. The rate is determined by the low probability for an end-standing molecule on a polymeric alcohol chain to find an appropriate donor or acceptor site on an adjacent chain. This process leads to a change in polarization, since the vectorial sum of the involved dipole moments will change markedly. Such a mechanism does not only apply to the alcohols, but also to N-methylformamide, water and formamide [20]. Due to the higher number of donor sites, which is reflected in the two-dimensional structure of formamide and the spacefilling network of water, cooperative process, τ_1, and molecular reorientation, τ_2, are not resolved and only two dispersion steps can be found. The short relaxation time of water, $\tau_2 = 1.02$ ps is close to the life time of a hydrogen bond, $\tau_{HB} = 0.54$ ps, deduced by Conde and Teixeira [27] from Rayleigh scattering experiments.

For the time constant of fast relaxing liquids an increasing frequency coverage may lead to a substantial change of τ. For instance, for acetonitrile the analysis of data up to 40 GHz suggests a Debye type relaxation with $\tau_1 = 3.48$ ps. When going up to $\nu_{max} = 89$ GHz the behaviour changes to a Cole-Cole distribution with $\tau_1 = 3.21$ ps due to the high dielectric loss in the E-Band region. Such an increased absorption at high frequencies, resulting in an asymmetric band shape, is also found for DMSO and propylene carbonate [20]. A reason for this excess loss may be the mechanism of cooperative adiabatic reorientation in clusters suggested by Gerschel et al. [14,15]; additional far-infrared data are necessary to clarify the problem.

THE INFLUENCE OF ELECTROLYTES ON SOLVENT PERMITTIVITY

Typical for electrolyte solutions is the lowering of the static solvent permittivity ε_s, specific for the dissolved electrolyte, Fig.5, which can usually be fitted to a polynomial of the type

$$\varepsilon_s(c) = \varepsilon_s(0) - \delta_\varepsilon \cdot c + \beta \cdot c^n; \quad n = 2 \text{ or } 3/2 \tag{12}$$

Besides volume effects (Φ), which may become important for salts with big ions such as tetrabutylammonium perchlorate in acetonitrile, Fig. 5b (curve 4), the dielectric depression is caused by irrotational bonding (IB) of the ions and by kinetic depolarization (KD). The theoretical concepts developed for the contributions of IB [28,29] and KD [30,31] apply at the limit of infinite dilution, so that data of good quality at low electrolyte concentrations are needed to determine reliable values of δ_ε for the discussion. Actually no unifying theory of the dielectric decrement is available, although a promising approach to this problem has been proposed by Patey and coworkers, see ref.[32] and literature quoted therein.

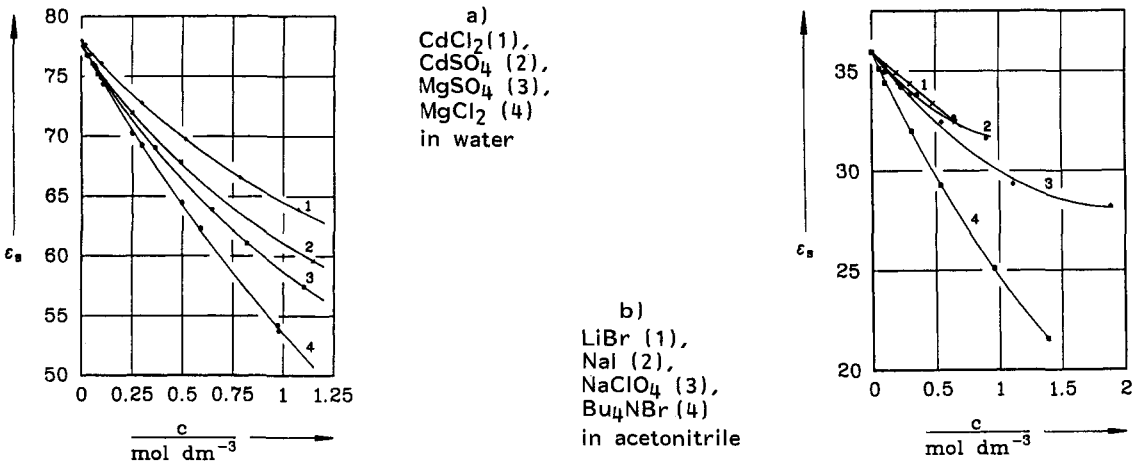

Fig. 5. Static permittivity of the solvent, ε_S, as a function of electrolyte concentration at 25°C

It is generally assumed that the aformentioned effects contribute additively to the experimental decrement

$$\delta_\varepsilon = \delta_\varepsilon^{\Phi} + \delta_\varepsilon^{IB} + \delta_\varepsilon^{KD} \qquad (13)$$

Kinetic depolarization arises from the opposite directions in which ion and surrounding point charges, making up the solvent dipoles, move in an external field. In the continuum theory of Hubbard and Onsager [33] the resulting torque on the dipoles leads to a decrease of solvent permittivity, $\Delta\varepsilon_S = \varepsilon_S(c) - \varepsilon_S(0)$, which is proportional to the specific conductance κ of the sample, and also to a decrease of ionic mobility. In an improved form of the theory [30], $\Delta\varepsilon_S$ can be written for a Debye-type relaxation of the solvent as follows

$$\Delta\varepsilon_s = \xi \cdot \kappa; \quad \xi = p \cdot \frac{\varepsilon_s(0) - \varepsilon_\infty(0)}{\varepsilon_s(0)} \cdot \frac{\tau_s(0)}{\varepsilon_o} \qquad (14)$$

The parameter p characterizes the hydrodynamic boundary conditions of slip (p=2/3) or stick (p=1) ionic movement. An extension to superimposed Debye processes such as found for mixed solvents and extensive tests on literature data of ionic mobilities were made by Ibuki and Nakahara [34,35]. According to eq.(14) the depolarization factor ξ of the continuum theory does not depend on the nature of the ion, in contrast to experimental results[5]. To overcome this problem Hubbard, Colonomos and Wolynes [30], suggested a microscopic theory which predicts a pronounced dependence of ξ on the ionic radius, with the slip result of eq.(14) as the limiting case for large radii. Actually only results for water and methanol are available. For a consistent discussion of δ_ε-data of various solvent systems we will therefore confine our analysis to the continuum approach.

Irrotational bonding is due to the high field strength in the vicinity of the ionic charge which leads to a symmetric polarization (dielectric saturation) of the surrounding solvent dipoles, resulting in a decrease of the number of molecules which are able to reorientation in the external field. This effect is correlated with solvation; however, "solvation numbers" obtained by this method are not necessarily equal to results from other methods, especially scattering data or computer simulations, since the directing force of the ion extends beyond the first coordination sphere.

According to Lestrade et al. [29], a solvation number Z_L can be calculated with the help of the relations

$$Z_L = (\rho - \rho_o + qc)/c; \quad q = \delta_\varepsilon^{st} \cdot \frac{\rho_o}{\varepsilon_s(0)} \cdot \frac{2\varepsilon_s^2(0) + \varepsilon_\infty^2}{(2\varepsilon_s(0) + \varepsilon_\infty)(\varepsilon_s(0) - \varepsilon_\infty)} \qquad (15a,b)$$

In eqs. (15) ρ is the number density of the solvent at electrolyte concentration c, ρ_o is the number density of the pure solvent. $\delta_\varepsilon^{st} = \delta_\varepsilon^{\Phi} - \delta_\varepsilon^{IB}$ is the dielectric decrement corrected for kinetic depolarization (see eq.(14)). Using slip boundary conditions, this approach yields a consistent series of ionic "Lestrade numbers" for the few electrolytes in methanol studied so far in the complete frequency range of our laboratory: $Z_L(COl\bar{4}) \approx 0$, $Z_L(Bu_4N^+) \approx 0$, $Z_L(NH_4^+) = 0$, $Z_L(Na^+) \approx 7$, and $Z_L(Br^-) \approx 7$. A Lestrade number of zero for the ammonium ion seems surprising, because this ion is able to form hydrogen bonds to the solvent, but our finding is corroborated by the relaxation times and infrared studies [36].

For aqueous solutions, again with p=2/3, Lestrade numbers $Z_L(Cl^-) \approx Z_L(ClO_4^-) \approx 0$, $Z_L(SO_4^{2-}) \approx 4$, $Z_L(Na^+) \approx 5$, $Z_L(Mg^{2+}) \approx 15$, and $Z_L(Cd^{2+}) \approx 12$ are obtained.

Figure 6 compares the effect of $NaClO_4$ on different solvents. In this graph the scaled static permittivity of the solvent, $\varepsilon_r = \varepsilon_S(c)/\varepsilon_S(0)$ is plotted against the relative concentration of the electrolyte, $c_r = c/c_S$; c_S is the molar concentration of the solvent. For all systems the high-

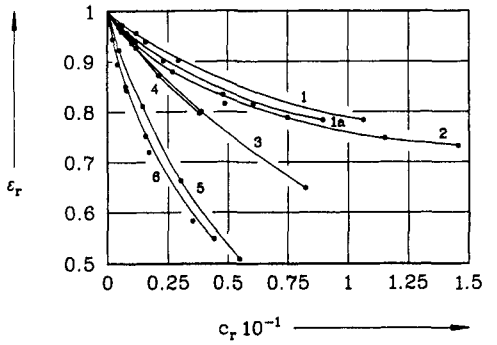

Fig. 6. Relative static permittivity of the solvent, $\varepsilon_r=\varepsilon_s(c)/\varepsilon_s(0)$, as a function of the relative concentration, $c_r=c/c_s$, of $NaClO_4$ at 25°C in acetonitrile (curve 1 without, curve 1a with ion-pair correction, cf. the text), propylene carbonate (2, taken from ref.[37]), DMF (3), formamide (4), methanol (5), and NMF (6).

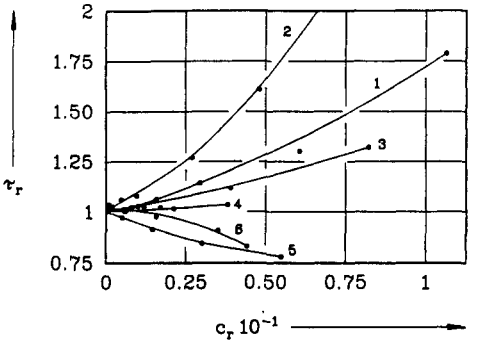

Fig. 7. Relative relaxation times of the main dispersion step, $\tau_r=\tau_{s1}(c)/\tau_{s1}(0)$, as a function of the relative concentration $c_r=c/c_s$ of $NaClO_4$ at 25°C in acetonitrile (curve 1), propylene carbonate (2, taken from ref.[37]), DMF (3), formamide (4), methanol (5), and NMF (6).

est electrolyte concentration is between one and two molar. Looking at the initial slopes, two "classes" of solvents can be distinguished.

The addition of electrolytes to solvents forming chains of hydrogen-bonded molecules, methanol (curve 5) and N-methylformamide (curve 6), causes a strong decrease of permittivity. At a molar ratio of electrolyte vs. solvent of 1:20 $\varepsilon_s(c)$ diminishes to about 50 % of the permittivity of the pure solvent, reflected by a high Lestrade number of $Z_L^{slip}=7.3$ for the methanol and $Z_L^{slip}=10.6$ for the NMF solution. Obviously a drastic breakdown of the solvent structure occurs, probably by a reduction of the average chain length, which - at least for the alcohol, since $Z_L^{slip}(ClO_4^-)\approx 0$ - is mainly due to the cation.

At the opposite extreme, the simple dipolar liquid acetonitrile (curve 1) is almost unaffected by the solute; a Lestrade number of $Z_L^{slip}=2.4$ is found. This may be due to the appreciable amount of contact ion pairs (CIP, $K_A=31$ dm mol^{-1}) which can be detected in this solvent, see chapter 7. If the concentration of free ions - this quantity is accessible from the ion-pair dispersion amplitudes - is used in the calculation of c_r, the initial slope of acetonitrile (curve 1a) is comparable to propylene carbonate (curve 2, $Z_L^{slip}=4.4$), dimethylformamide (curve 3, $Z_L^{slip}=4.6$), and formamide (curve 4, $Z_L^{slip}=4.3$). The similarity between PC (curve 2) and acetonitrile (curve 1a) persists up to high c_r values, where the permittivities of both solvents seem to level in the range of 0.7 $\varepsilon_s(0)$ to 0.8 $\varepsilon_s(0)$.

In a discussion of the concentration dependence of the main relaxation time τ_{s1}, hydrogen-bonding liquids must be distinguished from dipolar aprotic solvents. The latter usually exhibit only one dispersion step, eventually with a relaxation time distribution [19,20], and τ_{s1} increases monotonously with concentration. This is exemplified in Fig.7 for $NaClO_4$ solutions in acetonitrile (curve 1), propylene carbonate (curve 2), and DMF (curve 3), where the relative relaxation time $\tau_r=\tau_{s1}(c)/\tau_{s1}(0)$ is plotted against the relative electrolyte concentration $c_r=c/c_s$. At least for electrolyte concentrations below 0.5 M - but in some cases over the entire solubility range, e.g. LiNCS in DMSO [16] - the microscopic relaxation time of the solvent molecules τ'_{s1}, calculated with eq.(16), is proportional to the viscosity η of the solution for these systems. Such a behaviour is predicted by the modified Stokes-Einstein-Debye equation [38]

$$\tau' = \frac{3V}{kT} f_\perp C \cdot \eta \qquad (16)$$

for rotational diffusion of single molecules as the relaxation mechanism. In eq.(16), V is the molecular volume and $f_\perp$ is related to the ratio of the principal axes of the rotational ellipsoid representing the solvent molecule. The empirical factor C (C=1 for stick boundary conditions) couples the microscopic viscosity felt by the reorienting particle to macroscopic viscosity. From our dielectric relaxation studies on electrolyte solutions in the dipolar aprotic liquids propylene carbonate [37], DMSO, DMF, and acetonitrile, we obtain $C<0.1$ for all solvents. This suggests that the reorientational motion of the solvent molecules is much less affected by ion-solvent interactions than the viscous flow.

Due to its cooperative nature, the principal relaxation time of hydrogen-bonding liquids is intimately linked to the structure of these systems. From Figs.7 and 8 it is obvious, that the effect of added electrolyte depends both on the solvent (Fig.7) and on the nature of the solute (Fig.8). According to the few data available, τ_{s1} of N-methylformamide monotonously decreases with increasing electrolyte concentration [39,40,16], whereas for methanol solutions a maximum of $\tau_{s1}(c)$, although not very pronounced for sodium salts, seems to be characteristic [5,9,16] (cf.Fig.7, curves 5,6). This suggests that the long range order in these

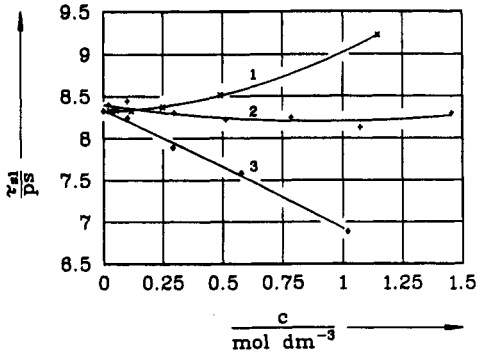

Fig. 8. Relaxation time of the main dispersion of water, τ_{s1}, as a function of electrolyte concentration at 25°C for $CdSO_4$ (curve 1), $CdCl_2$ (2), and $Cd(ClO_4)_2$ (3).

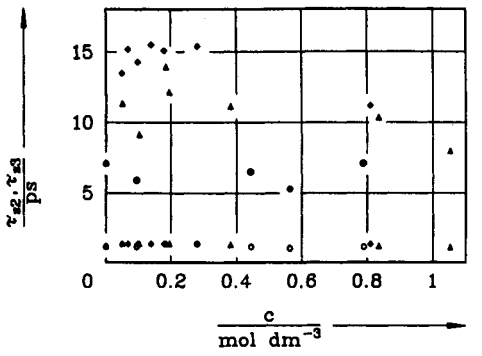

Fig. 9. Intermediate, τ_{s2} (closed symbols), and fast solvent relaxation time, τ_{s3} (open symbols), for methanol solutions of $NaClO_4$(Δ) Bu_4NClO_4 (◇), and NH_4Br(○) at 25°C.

solvents through winding hydrogen-bonded chains is broken up in the amide, whereas in the alcohol the bulk structure is relatively unaffected or even slightly stabilized at low concentrations. Such a result for the alcohol is corroborated by simulation studies of Jorgensen et al. [40], who find a strong interaction of the sodium ion with six solvent molecules in its primary coordination sphere, but no effect on the bulk structure beyond the first shell. At high c_r-ratios, the strong interaction of a Na^+-ion with six methanol molecules prevents the maintainance of the bulk solvent structure and the structure breaking effect of ion-solvent interactions dominates.

Formamide solutions exhibit either a slightly decreasing (NaI [40]) or increasing relaxation time $\tau_{s1}(c)$ ($LiNO_3$ [39], $NaClO_4$ [16], cf.Fig.7, curve 4). The relative change is smaller, about 10 % for 1 M solutions, than for dipolar aprotic and chain forming solvents; it is comparable to the behaviour of aqueous electrolytes, cf. Fig.8. Obviously, the cooperative dynamics of the two-dimensional (formamide) or three-dimensional (water) hydrogen-bonded networks is fairly insensitive to ion-solvent interactions in the concentration range studied; the same conclusion must be true for their structure. Figure 8 shows the influence of the cation on the cooperative dynamics of aqueous Cd-salt solutions. The increase of τ_{s1} for $CdSO_4$ or the constancy for $CdCl_2$, both salts undergoing strong ion-pair formation, in contrast to $Cd(ClO_4)_2$, is partially an effect of ion-pairing, but different rates for the solvent exchange between bulk and primary cation coordination sphere should be of similar importance. A consistent theory is still lacking.

Characteristic for all hydrogen-bonding liquids studied over a sufficiently large frequency range is the emergence of a fast relaxation process of Debye type centered in the 60 to 200 GHz region, which must be assigned to the dynamics of the hydrogen bond. The strongest argument that this process is due to specific solvent-solvent interactions is exemplified in Fig.9 for methanol. For all systems studied so far, the fast relaxation time τ_{s3} is specific for the solvent (1.02 ps for water, 1.12 ps for methanol, 0.78 ps for NMF, and 1.16 ps for formamide), but independent of the concentration and the nature of the dissolved electrolyte.

The intermediate relaxation times τ_{s2} of methanol, τ_{s2}=7.1 ps, and NMF, τ_{s2}=7.9 ps, are compatible with the reorientation of single molecules. For monomers a dependence on viscosity predicted by eq.(16) could be expected and this is indeed found for $NaClO_4$ solutions in NMF [16], in contrast to methanol solutions. Due to the small dispersion amplitude, the error in τ_{s2} may be in the order of 20 % (cf. the scatter of the $NaClO_4$-data in Fig.9). Nevertheless, a significant maximum of τ_{s2} at low electrolyte concentrations is found for all methanol solutions studied, except NH_4Br, where the relaxation time is constant. It must be concluded, that the intermediate relaxation process predominantly probes - at least for methanol - the motion of molecules situated at the ends of hydrogen-bonded chains and the solvent exchange in the solvation shell. This argument is corroborated by simulation studies [24] and results from vibrational spectroscopy [42,43], which find only a negligible concentration of monomers in the pure liquids. The fact, that the addition of ammonium bromide to methanol affects neither τ_{s2} nor the dispersion amplitude, together with arguments from vibrational spectroscopy [36], leads to the assumption that NH_4^+-methanol interactions and methanol-methanol interactions are of comparable magnitude and take place in the same time scale, governed by the lifetime of the hydrogen bond, hence yielding $Z_L(NH_4^+)$=0. The bromide ion is able to induce a symmetrical polarization of the solvent ($Z_L(Br^-)$≈7), with a residence time of a methanol molecule in the coordination sphere which is similar to its reorientation time.

ION-PAIR RELAXATION

For aqueous solutions of 1:2-, 2:2-, and 3:2-valent electrolytes it is well known that ion-pair (IP) formation gives rise to an additional relaxation process on the low-frequency side

of the solvent dispersion [28,44,45,7]. Such processes are also well known for 1:1 electrolytes in low-permittivity solvents, such as ethers, which are intensively studied by the groups of Petrucci [46] and Lestrade [29]. Recently ion-pair relaxation processes were also found for 1:1 electrolytes in solvents of permittivities ranging from 32 (methanol) to 46 (DMSO): Bu_4NBr [17], LiBr, NaI, and $NaClO_4$ in acetonitrile (AN), Bu_4NClO_4 in methanol and DMF, LiNCS in DMSO [16].

Figure 3 shows Argand diagrams of Bu_4NBr solutions in acetonitrile at two concentrations[17]; it represents the generalized complex permittivity η'' vs. ε' (curves 1 and 3), eqs.(9), and the diagram ε'' vs. ε' (curves 2 and 4) after conductance correction. The individual contributions (from left to right) of solvent relaxation, ion-pair relaxation, and conductances to the solution permittivity are indicated by broken lines.

Using Cavell's equation [47] with dipole moments μ_{IP} based on reasonable models for the ion pair, it is possible to determine the ion-pair concentration c_{IP} from the experimental dispersion amplitudes $\varepsilon-\varepsilon_2$, $\varepsilon_2=\varepsilon_s$

$$c_{IP} = \frac{2\varepsilon+1}{3\varepsilon} \cdot \frac{3kT\varepsilon_o}{10^{-3}N_A} \cdot \frac{(1-\alpha_{IP}f_{IP})^2}{\mu_{IP}^2} \cdot (\varepsilon-\varepsilon_2) \qquad (17)$$

In this equation α_{IP} is the polarizability and f_{IP} is the reaction field factor of the ion pair. Comparing association constants K_A estimated with the c_{IP}-data of the tested ion-pair models with literature values K_A^{Lit} obtained by conventional methods, like calorimetric or conductance studies, allows the identification of the polar species formed [49]. Some results are summarized in Table 2, where CIP stands for contact and SSIP for solvent-shared ion pairs.

Except for $NaClO_4$ solutions in methanol, where the scattering of the data is large, due to the very small IP dispersion amplitudes, additional information is available from the relaxation times $\tau_{IP}(c)$. Assuming rotational diffusion as the predominating relaxation mechanism of the ion pair, an increase of τ_{IP} with concentration must be expected, since the viscosity increases with increasing electrolyte concentration. Such a behaviour is found for LiNCS/DMSO and LiBr/AN solutions; data analysis reveals contact ion pairs as the relaxing species.

Surprisingly, an initial decrease of the ion-pair relaxation time with increasing concentration was found for the majority of the investigated systems: Bu_4NBr, NaI, $NaClO_4$ in AN, and $NaClO_4$ in DMF, $MgSO_4$, $CdSO_4$, $CdCl_2$ in water, with a minimum of τ_{IP} around 0.5 M to 1M. This leads to the assumption that the kinetics of ion-pair formation

$$C^{z+} + A^{z-} \underset{k_{21}}{\overset{k_{12}}{\rightleftharpoons}} (IP)^{z+ +z-} \qquad (18)$$

controlled by the rate constants of formation, k_{12}, and decomposition, k_{21}, contribute to the experimental relaxation times. An equation can be derived [51,52], which predicts a linear dependence of the relaxation rate τ_{IP}^{-1} on the concentration of free ions, $(c-c_{IP})$

$$\tau_{IP}^{-1} = (\tau_{IP}')^{-1} + k_{21} + 2k_{12}(c - c_{IP}) \qquad (19)$$

The first term on the right side of eq.(19), τ_{IP}' is the single particle correlation time of the rotating ion pair; the second term is the relaxation time of the kinetic mode given by the kinetic time law underlying eq.(18). Indeed, this equation is reasonably followed up to the concentration of relaxation time minimum. The rate constants of formation, k_{12}, obtained from the slopes are given in Table 2, together with the rate constants of decomposition $k_{21}=k_{12}/K_A$ calculated with the help of ion-pair association constants from the dispersion amplitudes of the ion-pair relaxation process. In all cases, τ_{IP}' obtained from eq.(19) is compatible only with that type of ion pair controlling the dispersion amplitude.

Table 2: Association and rate constants of ion-pair formation from dielectric relaxation data at 25° C.

solvent	electr.	IP	K_A	$K_A^{Lit.}$	$k_{12}\cdot10^{-9}$	$k_{21}\cdot10^{-9}$
			dm^3mol^{-1}		$dm^3mol^{-1}s^{-1}$	s^{-1}
water	$MgSO_4$	SSIP	164±25	156[48]	1.8±0.1	0.011±0.001
	$CdSO_4$	SSIP	270±90	245[49]	2.3±0.4	0.009±0.002
AN	LiBr	CIP	148±2	155-193[b)]	a)	
	NaI	CIP	17±6	3.8-24[b)]	8±1	0.4±0.1
	$NaClO_4$	CIP	31±3	15-27[b)]	10.7±0.4	0.44±0.04
DMF	$NaClO_4$	SSIP	1.9±1.3	3.2±0.7[50]	4.7±0.2	1.5±0.3

a) τ_{IP} constant b) re-analysis of conductance data from the literature

CONCLUSIONS

Important information, not accessible by other techniques, can be obtained when dielectric relaxation spectroscopy of high accuracy is applied over a wide frequency range. For electrolyte solutions and their solvents, the technique can successfully be used to probe structural effects and especially the dynamics of ion-ion, solvent-solvent and ion-solvent interactions. Actually, the 0.9 to 89 GHz range accessible with the equipment of our laboratory still limits investigations to selected solvents and prevents the study of the features outside this frequency range, but we will overcome this restriction in the near future with new equipment under construction.

Acknowledgement We are grateful to the Deutsche Forschungsgemeinschaft for a generous support of our investigations.

REFERENCES

1. A. Gerschel, in: A.J. Barnes, W.J. Orville-Thomas, and J. Yarwood (eds.), Molecular Liquids - Dynamics and Interaction, Nato ASI, Ser.C, 135, 163-199, Reidel, Dordrecht (1984).
2. B. Bagchi, Annu. Rev. Phys. Chem. 40, 115-141 (1989).
3. E.H. Grant, R.J. Sheppard, and G.P. South, Dielectric Behaviour of Biological Molecules in Solution, Oxford University Press (Clarendon), London (1978).
4. S. Mashimo, S.Kuwabara, S. Yagihara, and K. Higasi, J. Phys. Chem. 91, 6337-6338(1987).
5. J. Barthel and R.Buchner, Pure Appl. Chem. 58, 1077-1090 (1986).
6. J. Barthel, K.Bachhuber, and R. Buchner, in: M. Moreau and P. Turq (eds.),Chemical Reactivity in Liquids - Fundamental Aspects, Plenum Press, New York, 55-71 (1988).
7. J. Barthel, R. Buchner, and H. Steger, Wiss. Zeitschr. THLM 31, 409-423 (1989).
8. R.H. Cole, Annu. Rev. Phys. Chem. 28, 283-300 (1977).
9. R.H. Cole, J.G. Berberian, S. Mashimo, G. Chryssikos, A. Burns, and E. Tombari, J. Appl. Phys. 66, 793-802 (1989).
10. C.F.J.Böttcher and P. Bordewijk, Theory of Electric Polarization 2 (2nd ed.), Elsevier, Amsterdam (1978).
11. U. Kaatze and K.Giese, J. Phys. E: Sci. Instrum. 13, 133-141 (1980).
12. J.R. Birch, G.P. O'Neill, J. Yarwood, and M. Bennouna, J. Phys. E.: Sci. Instrum. 15, 684-688 (1982).
13. Y.-Z. Wei and S. Sridhar, Rev. Sci. Instrum. 60, 3041-3046 (1989).
14. A. Gerschel, T. Grochulski, Z. Kisiel, L.Pszczolkowski, and K. Leibler, Mol. Phys. 54, 97-117 (1985).
15. A. Gerschel, J. Chim. Phys. 86, 1857-1869 (1989).
16. unpublished results from the authors' laboratory
17. J. Barthel and M. Kleebauer, J. Solution Chem., in press.
18. J. Barthel, H.J. Gores, G. Schmeer, and R. Wachter, in: F.L. Boschke (ed.), Topics in Current Chemistry 111, 35-144, Springer Verlag, Heidelberg (1983).
19. J. Barthel, K. Bachhuber, R. Buchner, and H. Hetzenauer, Chem. Phys. Lett. 165, 369-373 (1990).
20. J. Barthel, K. Bachhuber, R. Buchner, B. Gill, and M. Kleebauer, Chem. Phys. Lett. 167, 62-66 (1990).
21. B. Kaukal, PhD-Thesis, Regensburg (1982).
22. R. Buchner and J. Yarwood, Mikrochim. Acta 2, 335-337 (1988).
23. S.K. Garg and C.P. Smyth, J. Phys. Chem. 69, 1294-1301 (1965).
24. M. Haughney, M. Ferrario, and I.R. McDonald, J. Phys. Chem. 91, 4934-4940 (1987).
25. H. Versmold, Ber. Bunsenges. Phys. Chem. 84, 168-173 (1980).
26. F.J. Bermejo, F. Batallán, E. Enciso, R. White, A.J. Dianoux, and W.S. Howells, J. Phys.: Condens. Matter 2, 1301-1314 (1990).
27. O. Conde and J. Teixeira, J. Phys. (Paris) 44, 525-529 (1983).
28. U. Kaatze, Z. Phys. Chem. NF 135, 51-75 (1983).
29. J.-P. Badiali, H. Cachet, and J.-C. Lestrade, Pure Appl. Chem. 53, 1383-1399 (1981).
30. J.B. Hubbard, P. Colonomos, and P.G. Wolynes, J. Chem. Phys. 71, 2652-2661 (1979).
31. B.U. Felderhof, Mol. Phys. 51, 801-811 (1984).
32. P.G. Kusalik and G.N. Patey, J. Chem. Phys. 88, 7715-7738 (1988).
33. J.B. Hubbard and L. Onsager, J. Chem. Phys. 67, 4850-4857 (1977).
34. K. Ibuki and M. Nakahara, J. Chem. Phys. 84, 2776-2783 (1986); ibid 84, 6979-6983 (1986).
35. K. Ibuki and M. Nakahara, J. Phys. Chem. 91, 1864-1867, 4411-4414, 4414-4416 (1987).
36. J. Barthel and A. Schramm, unpublished results.
37. J. Barthel and F. Feuerlein, J. Solution Chem. 13, 393-417 (1984).
38. J.C. Dote, D. Kivelson, and R.N. Schwartz, J. Phys. Chem. 85, 2169-2180 (1981).
39. J. Barthel, H. Behret, and F. Schmithals, Ber. Bunsenges. Phys. Chem. 75, 305-309 (1972).
40. P. Winsor, IV, and R.H. Cole, J. Phys. Chem. 86, 2486-2490 (1982).
41. W.L. Jorgensen, B. Bigot, and J. Chandrasekhar, J. Amer. Chem. Soc. 104, 4584-4591(1982).
42. G. Kabisch and K. Pollmer, Z. Phys. Chem. Leipzig 266, 687-694 (1985).
43. W.A.P. Luck and W. Ditter, Ber. Bunsenges. Phys. Chem. 72, 365-374 (1968).
44. U. Kaatze, V. Lönnecke, and R. Pottel. J. Phys. Chem. 91 2206-2211 (1987).
45. U. Kaatze and K. Giese, J. Mol. Liquids 36, 15-35 (1987).
46. M. Xu, N. Inoue, E.M. Eyring, and S. Petrucci J. Phys. Chem. 92, 2789-2798 (1988).
47. E.A.S. Cavell, P.C. Knight, and M.A.Sheikh, J. Chem. Soc. Faraday Trans. 67, 2225-2233 (1971).
48. J. Barthel and H.-J.Wittmann, unpublished results.
49. J. Barthel, R. Buchner, and H.-J. Wittmann, Z. Phys. Chem. NF 139, 23-37 (1984).
50. B.S. Krumgalz and J. Barthel, Z. Phys. Chem. NF 142, 167-178 (1984).
51. J.E.Anderson, J. Chem. Phys. 51, 3578-3581 (1969).
52. J.E. Anderson, Ber. Bunsenges. Phys. Chem. 75, 294-296 (1971).